INTERNATIONAL JOURNAL FOR NUMERICAL METHODS IN FLUIDS, VOL. 16, 391–401 (1993)

INDENTED PLATE PROBLEM REVISITED

TUNCER CEBECI*, HSUN H. CHEN† AND JUDITH A. MAJESKI‡

Aerospace Engineering Department, California State University, Long Beach, CA 90840, U.S.A.

SUMMARY

An interactive boundary layer method, together with the e^n approach to the calculation of transition, has been used to investigate the flow over an indented surface for which previous calculations had led to numerical instabilities. The results show two possible reasons for these numerical difficulties. First, it is shown that the gradients of wall shear become very steep at larger Reynolds numbers, particularly in the vicinity of reattachment. Extremely fine numerical grids are required to resolve these gradients. Secondly, and perhaps of greater importance, transition is shown to occur within the region of recirculation for all Reynolds numbers except for the lowest ones. Thus, the calculated flows downstream of the transition locations are fictitious and may be expected to deviate from the corresponding real flows by increasing amounts as the Reynolds number becomes larger. Calculations involving laminar, transitional and turbulent flow have been performed and confirm this conjecture.

KEY WORDS Laminar Turbulent Transitional flows Separation Reattachment Transition location

1. INTRODUCTION

It is well known that the laminar boundary layer equations can be solved for a prescribed pressure distribution as long as the flow remains attached and their solutions are independent of the Reynolds number. At the location of flow separation, defined to correspond to the vanishing of wall shear in steady flows, the solutions break down and this situation is sometimes referred to as the singular behaviour of the boundary layer equations at separation. There are no real solutions downstream of separation; the normal velocity component v becomes infinite at the separation point, x_s and, near x_s, the behaviour of the wall shear τ_w is of the form

$$\left(\frac{\partial u}{\partial y}\right)_w \propto (x_s - x)^{1/2}. \tag{1}$$

The boundary layer equations are not singular at separation, however, when the external velocity or pressure is computed as part of the solution. Catherall and Mangler[1] were the first to show that modifications of the external velocity distribution near the region of flow separation leads to solutions free of numerical difficulties. Prescribing the displacement thickness as a boundary condition, that is,

$$\delta^*(x) = \text{given}, \tag{2}$$

* Professor and Chairman.
† Associate Professor.
‡ Graduate Student.

0271–2091/93/050391–11$10.50

Received 13 August 1991
Revised 14 September 1992

in addition to the usual boundary conditions used to solve the boundary layer equations for a prescribed pressure distribution, they were able to integrate the boundary layer equations through the separation location and into a region of reverse flow without any evidence of a singular point. Their study has led to other studies by various investigators,[2-9] in which the solutions of the boundary layer equations were obtained for flows with and without separation by prescribing either displacement thickness or wall shear distributions. This technique, which is known as an inverse method, has also been used to develop numerical methods to solve the boundary layer equations with large regions of flow separation for a range of Reynolds numbers.[9,10] These studies considered laminar flows, and the question of whether the flows at these relatively high Reynolds numbers exist was not addressed.

Another inverse method designed to couple the solutions of the inviscid flow and boundary layer equations is the Hilbert integral procedure, proposed by Veldman.[11] In this approach, the value of external velocity $u_e(x)$ is written as the sum of the inviscid velocity, $u_e^0(x)$, and a perturbation velocity, $\delta u_e(x)$, to account for the viscous effects, that is,

$$u_e(x) = u_e^0(x) + \delta u_e(x), \tag{3}$$

with $\delta u_e(x)$ computed from the so-called Hilbert integral

$$\delta u_e(x) = \frac{1}{\pi} \int_{x_a}^{x_b} \frac{d}{d\sigma}(u_e \delta^*) \frac{d\sigma}{x-\sigma}, \tag{4}$$

where the interaction region is confined to (x_a, x_b). For a specified $u_e^0(x)$ and Reynolds number, the boundary layer equations are solved in the inverse mode simultaneously in successive sweeps over the given body until the solutions converge.

The Hilbert integral approach provides a relationship between external velocity $u_e(x)$ and displacement thickness $\delta^*(x)$ and is similar to the specified displacement thickness approach indicated by equation (2), which also provides such a relationship. However, there is an imporant difference in that, for the specified δ^*-case, the solutions of the boundary layer equations are obtained for one sweep on the body in contrast to the Hilbert integral approach which requires several sweeps. Since the solutions of the laminar boundary layer equations with separation depend on the Reynolds number, the Hilbert integral approach allows us to examine the behaviour of the solutions at each sweep and their approach to convergence. Typical useful studies include flows with large flow separation and their associated numerical difficulties and the accuracy and the convergence of the solutions at the reattachment point if the flow separates and reattaches. An approach based on the displacement thickness, which is not as versatile as the Hilbert integral approach, can provide most of this useful information but does not address the question of the convergence of the solutions at the reattachment point. It is also possible that this approach may not signal difficulties in achieving the solutions since the calculations do not bring in the downstream effects. The Hilbert integral approach, on the other hand, can signal potential difficulties since sweeps on the body bring the downstream effects into the calculations. The difficulties may be numerical or physical and their identification may not be an easy task.

In this paper, we consider a flow investigated by Henkes and Veldman[12] and speculate on the reasons for the difficulties observed in obtaining laminar flow solutions over the indented plate shown in Figure 1. The shape of the indented plate is given by

$$y_w = -0{\cdot}03 \operatorname{sech}4(\xi - 2{\cdot}5), \quad \xi \geq 0. \tag{5}$$

The problem was originally addressed by Carter and Wornom,[10] who presented solutions at a Reynolds number, $R = 8 \times 10^4$, over the interval $1 \leq \xi \leq 4$. Veldman[13] solved the problem at a Reynolds number of $R = 3{\cdot}6 \times 10^5$, but could not obtain converged solutions for larger Reynolds

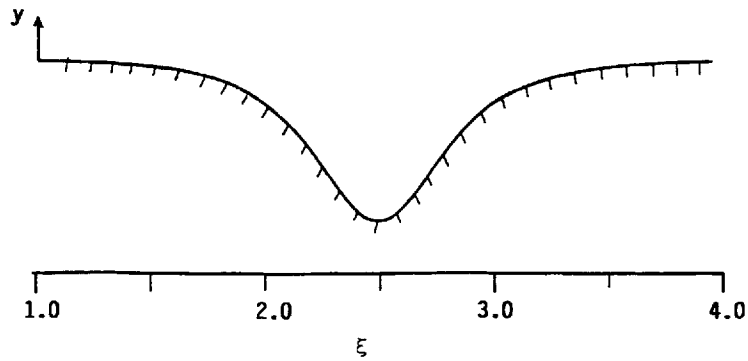

Figure 1. Indented plate problem

numbers. Both investigations used interactive boundary layer equations. A further attempt was made by Veldman and Dijkstra,[14] who treated the problem in a triple-deck framework and encountered difficulties at Reynolds numbers slightly above $3{\cdot}60 \times 10^5$. Careful iteration, using results at smaller Reynolds numbers as initial guesses, did not lead to success. Thus, two different steady descriptions of the flow problem experienced difficulties in almost the same situation. Henkes and Veldman stated that 'this gave the impression that something fundamental was going on: perhaps a steady solution does not exist at these large Reynolds numbers'.

Recently, Edwards and Carter[15] were able to calculate a steady solution at $R = 6 \times 10^5$ using a first-order scheme and neglecting the convective term in the x-direction in regions with backflow (FLARE approximation). Henkes and Veldman[12] also conducted studies at this Reynolds number with first-order solutions at $R = 6 \times 10^5$ as an initial guess, and stated that, 'it appeared possible to obtain the steady solution with a second-order scheme, without neglect of any terms, at this Reynolds number'. They also stated that solutions at larger Reynolds numbers could be obtained only by following an unsteady approach, starting from the steady solution at $R = 6 \times 10^5$; the steady solution at $R = 1{\cdot}5 \times 10^6$ was reached by increasing the Reynolds number as

$$R(t) = R_1 - (R_1 - R_0)\,\mathrm{sech}(t), \tag{6}$$

with $R_0 = 6 \times 10^5$, $R_1 = 1{\cdot}5 \times 10^6$.

As a rule, three sweeps were made at each time level. The almost steady solution on the 61×41 spatial grid at $t = 8{\cdot}0$, after 75 time steps, was used to initiate a calculation with the steady equations for $R = 1{\cdot}5 \times 10^6$ and an additional 58 sweeps were required to satisfy the criterion that the maximum norm of changes in $u_e\delta^*$ was below 10^{-4}. At $R = 1{\cdot}5 \times 10^6$, the 61×41 numerical grid resolved some of the details of the free-shear layer, and the wall shear stress of Figure 2 already shows some 'wiggles' between $\xi = 2{\cdot}0$ and $2{\cdot}5$, caused by a lack of resolution. Larger Reynolds numbers would require a finer grid, with increased computational cost.

Based on the above study, Henkes and Veldman concluded that 'at this depth of the indentation, the interacting boundary layer equations do have a steady solution at arbitrarily large Reynolds numbers. The difficulties encountered in the previous investigations seem to be of a numerical nature'.

More recently, Rubin and Himansu[16] examined the convergence properties of an iterative solution technique for the reduced Navier–Stokes equations for this flow. Techniques for decreasing the sensitivity to the initial pressure approximation, for fine meshes in particular, were

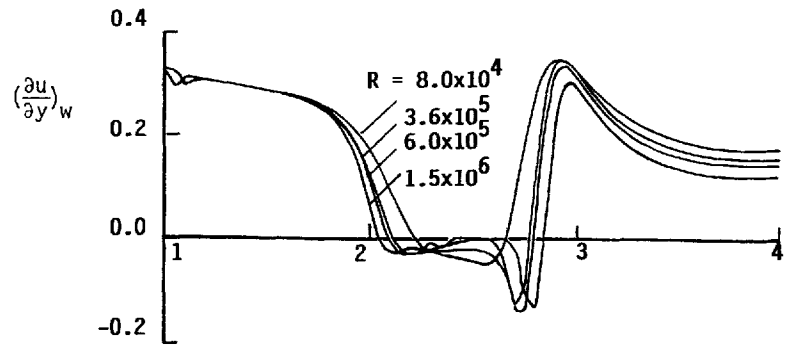

Figure 2. Wall shear stress of steady interacting boundary layer solution along an indented plate

investigated. Sufficient spatial grid refinement led to a shock-like attachment and, for sufficiently large Reynolds number, to a local 'divergence' of the numerical computations. Rubin and Himansu stated that this 'laminar flow breakdown' appeared to be related to an instability that is associated with high-frequency fine-grid modes that were not resolvable with their modelling. They conjectured that this behaviour might be indicative of dynamic stall or of incipient transition and that the instability was of a physical, rather than of a numerical, character.

In the present study, we examine the veracity of their conclusion at these high Reynolds numbers in the light of a recent study on laminar separation bubbles conducted by Cebeci[17] for a different problem but for a similar reason: Do the solutions of laminar boundary layer equations exist at high Reynolds numbers in the presence of separation and do the observed numerical instabilities have their origin elsewhere than in the numerical solution method? To elaborate on this point, it is useful to review Cebeci's study conducted for a leading edge of a thin ellipse at a reduced incidence angle of ξ_0. The study used the interaction formula provided by equations (3) and (4) and showed that the laminar boundary layer near the leading edge behaved well for $R = 10^5$, and was unseparated if the reduced incidence angle ξ_0 is less than $\xi_s = 1{\cdot}275$, although there was a significant adverse pressure gradient. At higher values of ξ_0, however, separation occurred and increased in its extent with increasing values of ξ_0. For ξ_0 up to 1·294, the solutions in the separated region behaved well, exhibited no numerical problems and the extent of the separation bubble which changed slowly with each sweep for a specified value of ξ_0, settled down after around 10 sweeps. The location of separation and the reattachment point remained constant with additional sweeps and the solutions indicated complete convergence in the entire flow field. When the same calculations were repeated for $\xi_0 = 1{\cdot}296$, however, the extent of the separation bubble began to grow with iteration and even though the loation of the onset of separation location remained essentially the same at each sweep, the reattachment point began to drift slowly with the number of sweeps. When calculations were repeated for $\xi_0 = 1{\cdot}298$, the results exhibited a similar behaviour as for $\xi_0 = 1{\cdot}296$ except that the drift in the reattachment location was more pronounced with sweep number. In both cases, however, there were no numerical problems and the inverse method was able to deal with increasing regions of flow separation until the separation bubble became so large that the reattachment point coincided with the end of the plate. At that point, the calculations had to be terminated since the solution of the Hilbert integral required downstream boundary conditions.

Possible reasons for the behaviour of the numerical instability in the calculation of the separation bubble was investigated by using the e^n-method based on the linear stability theory.

The computed transition locations obtained for values of reduced incidence ξ_0 up to 1·296 showed that transition moved forward with increasing ξ_0, with transition occurring almost at the reattachment point for $\xi_0 = 1{\cdot}290$ and moving inside the separation bubble at higher values of ξ_0. While for $\xi_0 < 1{\cdot}296$, the reattachment location of the separation bubble and the location of the onset of transition remained constant with the number of sweeps and the solutions converged: for $\xi_0 \geq 1{\cdot}296$, the extent of the separation bubble began to increase with the number of sweeps and caused the onset of transition to move upstream with each sweep. These results implied that the real flow was turbulent and had a shorter recirculation region, which was consistent with experiments and with the study of Cebeci and Schimke[18] and Cebeci,[19] who, in the calculation of long separation bubbles on aerofoils, observed a similar numerical instability and stated that reattachment and transition locations were related. Attempts to perform calculations with transition locations further downstream than those reported experimentally revealed a similar tendency for the reattachment location to move downstream with the number of sweeps used in the interactive procedure.

In the present study, in Section 2, we present results obtained with a calculation method based on a combination of an interactive boundary layer and stability-transition approach for the indented plate problem at low and high Reynolds numbers and conjecture on the conclusions reached by Henkes and Veldman[12] and Rubin and his co-workers[16,20,21] in the light of Cebeci's study.[19] The paper ends with a summary of the more important findings.

2. RESULTS AND DISCUSSION

The calculation method involves an interactive boundary layer method (IBL) and a transition prediction method based on the e^n method described by Cebeci.[19] The interactive method is based on the solution of the continuity and momentum equations for a two-dimensional incompressible flow, together with a Hilbert integral formulation which couples the boundary layer solutions to inviscid flow solutions appropriate to the indentation given by equation (5). It has been used in the calculation of many flows, so that its numerical features are known to be reliable and accurate. Where calculations were performed in regions of transitional and turbulent flow, the eddy viscosity formulation of Cebeci and Smith[22] was used and, again, is known from extensive examinations to be reliable.[23]

The results are presented in three sections. The first is concerned with the nature of the laminar flow solutions in the separated flow region and the extent to which they are influenced by Reynolds number and numerical grid resolution. The second is concerned with the determination of the location of the onset of transition, and of the extent to which this may obviate the need to deal with the first problem. In this case, the interactive scheme is used in conjunction with the e^n method. The third is concerned with laminar, transitional and turbulent flows and the extent to which they are influenced by the Reynolds number and the location of transition.

2.1. Interactive flow calculations

Results have been obtained for Reynolds numbers of 8×10^4, 2×10^5, $3{\cdot}6 \times 10^5$, 5×10^5 and 6×10^5 and are presented here in the form of the variation of wall shear parameter f''_w with distance ξ. In each case, a series of calculations was performed to show the influence of grid resolution and the number of sweeps required for convergence.

Figure 3 shows the results for the lowest Reynolds number. In this case, 50 uniformly distributed ξ-stations in the interval $1 \leq \xi \leq 4$ yielded results identical to those obtained with 100 and 200 ξ-stations. Also, convergence was achieved after 25 sweeps. Figure 3 shows that the wall

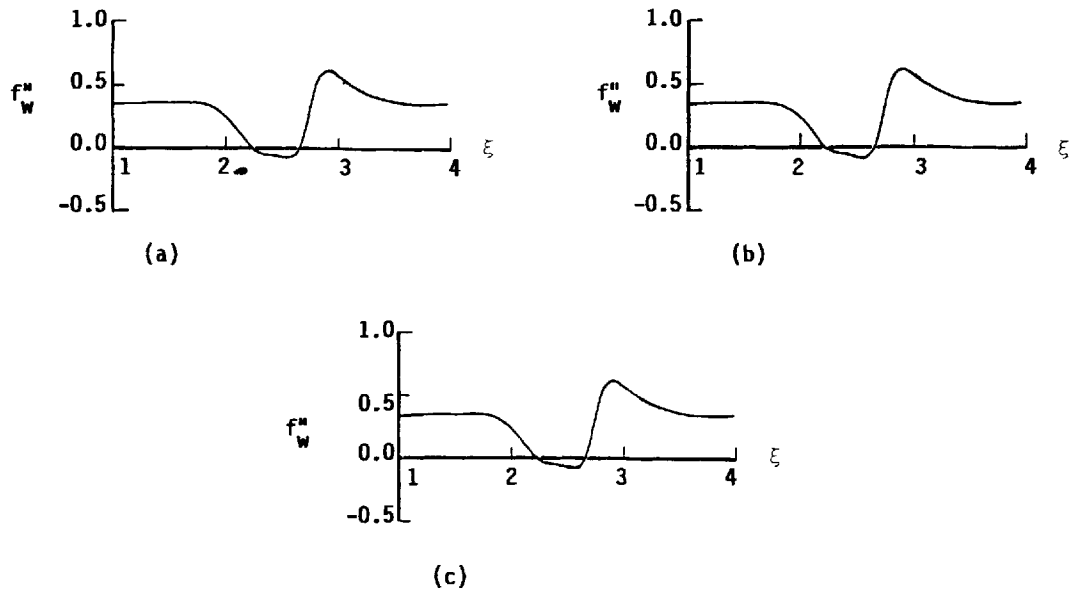

Figure 3. Variation of dimensionless wall shear parameter, $R_0 = 8 \times 10^4$: (a) $NX = 50$; (b) $NX = 100$; (c) $NX = 200$

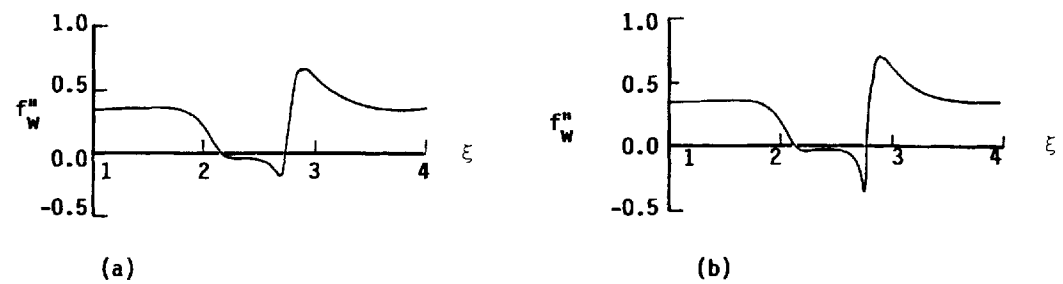

Figure 4. Variation of dimensionless wall shear parameter, $NX = 200$: (a) $R_0 = 2 \times 10^5$; (b) $R_0 = 3.6 \times 10^5$

shear decreases through separation to a minimum value, after which it increases gradually to zero at reattachment and continues to a maximum positive value before decreasing again to its asymptotic flat plate result.

At a Reynolds number of 2×10^5, calculations with 50 and 100 ξ-stations produced slight oscillations in the solutions and 200 uniformly distributed ξ-stations were required. Convergence was obtained after 40 sweeps. The results of Figure 4(a) show the variation of the wall shear parameter and that the gradients, particularly after the minimum value, are noticeably steeper than those of Figure 3(c). Figure 4(b) corresponds to a Reynolds number of $3{\cdot}6 \times 10^5$ and it can be seen that the minimum value of f''_w has moved downstream so that the gradients have become even more steep but are still able to be represented by 200 ξ-stations with convergence after 50 sweeps.[24] At a Reynolds number of 5×10^5, calculations show that the gradient of wall shear at the reattachment location is appreciably steeper and increases with each sweep. At sweep 32, the minimum and maximum values of f''_w occur at neighbouring grid locations and the sudden change in f''_w from a negative value to a large positive value causes the solutions to oscillate at subsequent

grid points. These oscillations progressively influenced the results of subsequent sweeps until the solutions broke down at a sweep number of 37. A closer look at the variation of the wall shear parameter[24] indicates that the solutions begin to oscillate at the 17th sweep. At the highest Reynolds number of 6×10^5, the situation was similar to that at 5×10^5 except that the minimum and maximum values of f''_w were achieved at neighbouring grid locations after only 20 sweeps, with consequent breakdown shortly thereafter. In this case, solutions began to exhibit oscillations after 13 sweeps, during which the reattachment point changed slowly.

These results show that the gradient of f''_w at the reattachment point achieves a near-infinite value at a Reynolds number greater than 5×10^5. This gradient can certainly be represented with a local increase of grid points but it can equally be expected that the subsequent oscillations will remain even with this increased cost of calculation. It seems, from a physical viewpoint, that this gradient is unreasonable; having shown the influence of Reynolds number, number of ξ-stations and sweeps, we now turn to examine the second possibility, namely, that of a flow which undergoes transition as a consequence of the region of separation.

2.2. Stability transition calculations

A summary of the calculated values of the locations of laminar separation and transition is given in Table I. The location of the reattachment is also shown but it should be remembered that this corresponds to a laminar flow even though we have determined that, except at a Reynolds number of 8×10^4, the onset of transition occurs either within or ahead of the separation bubble. These results, which are shown in Figure 5, were obtained with the e^n method, which led to the integrated amplification rates as a function of frequency and for the five values of Reynolds number shown in Table I.

The table shows that the lowest Reynolds number flow does not undergo transition over the ξ-distance considered. Thus, we have a laminar separation followed by a laminar reattachment and no difficulties with the numerical calculations. At a Reynolds number of 2×10^5, the calculations indicate that the onset of transition occurs upstream of the minimum value of the wall shear parameter, so that a substantial part of the calculated result of f''_w in Figure 5(b) corresponds to a laminar flow which may not be able to exist. The same pattern is evident at higher Reynolds numbers, where it is increasingly difficult to be certain that the correct value of n has been chosen. The results shown in Table I were obtained for a value of $n=9$, but lower values of n could lead to the occurrence of transition at or before the laminar separation location. Thus, it is reasonable to expect increasing numerical difficulties with the calculations of laminar flows which may not exist in practice and which correspond to larger regions of the flows considered here as the Reynolds number is increased.

Table I. Separation, reattachment, and transition location for laminar flow over an indented plate

R_0	Separation location	Reattachment location	Transition location
8×10^4	2·24	2·64	—
2×10^5	2·16	2·72	2·24
$3{\cdot}6 \times 10^5$	2·14	2·76	2·15
5×10^5	2·12	2·78	2·12
6×10^5	2·12	2·80	2·10

In spite of the near concurrence of laminar separation and transition for three of the cases of Table I, we can expect that the consequent turbulence effects will increase in importance with Reynolds number. This implies that the higher the Reynolds number, the more fictitious the laminar result will be and deviate from that which will occur in practice.

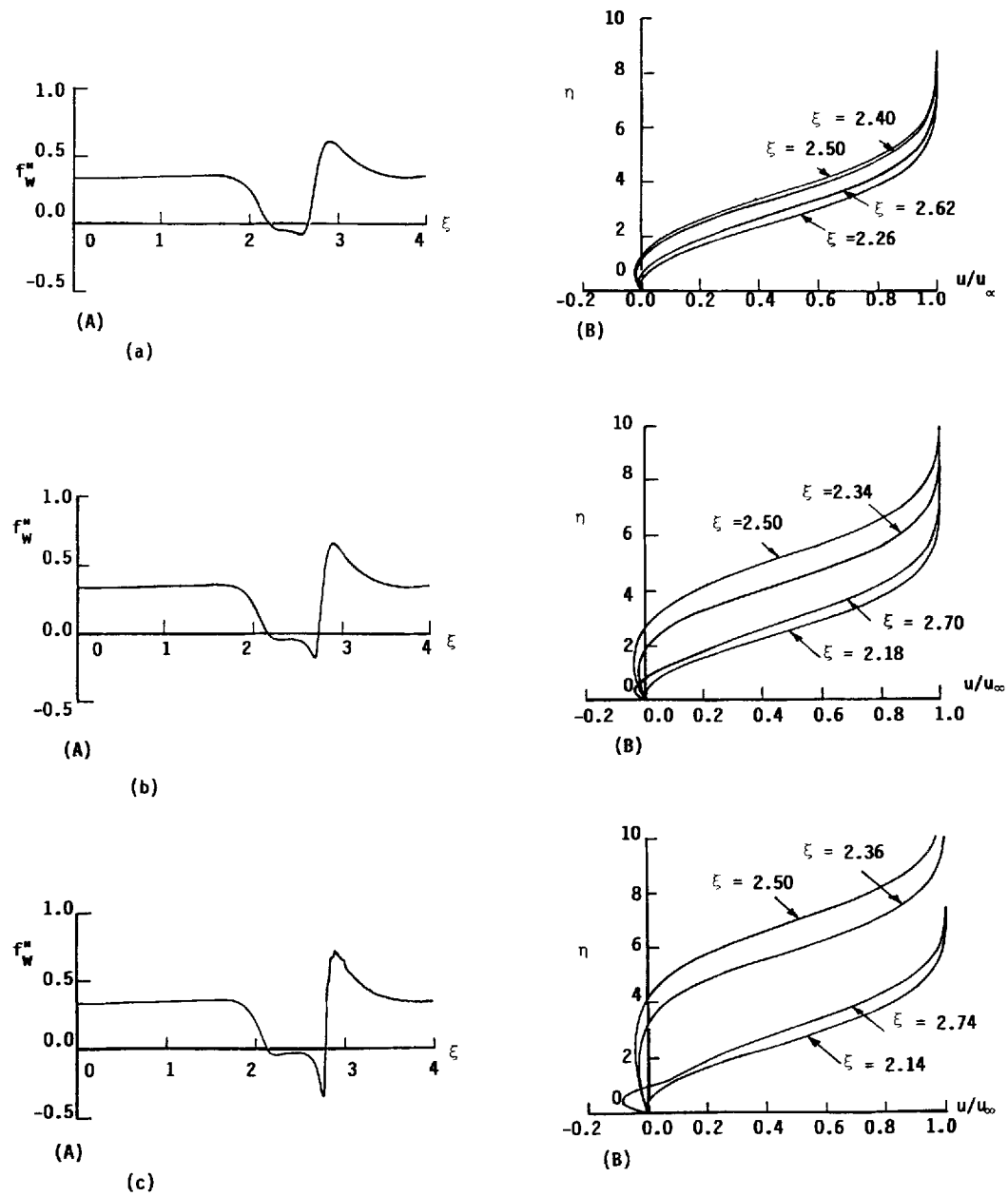

Figure 5. Variations of the (A) the dimensionless wall shear parameter, and (B) the dimensionless velocity profiles in the separation region: (a) $R_0 = 8 \times 10^4$; (b) $R_0 = 2 \times 10^5$; (c) $R_0 = 3.6 \times 10^5$; (d) $R_0 = 5 \times 10^5$; (e) $R_0 = 6 \times 10^5$

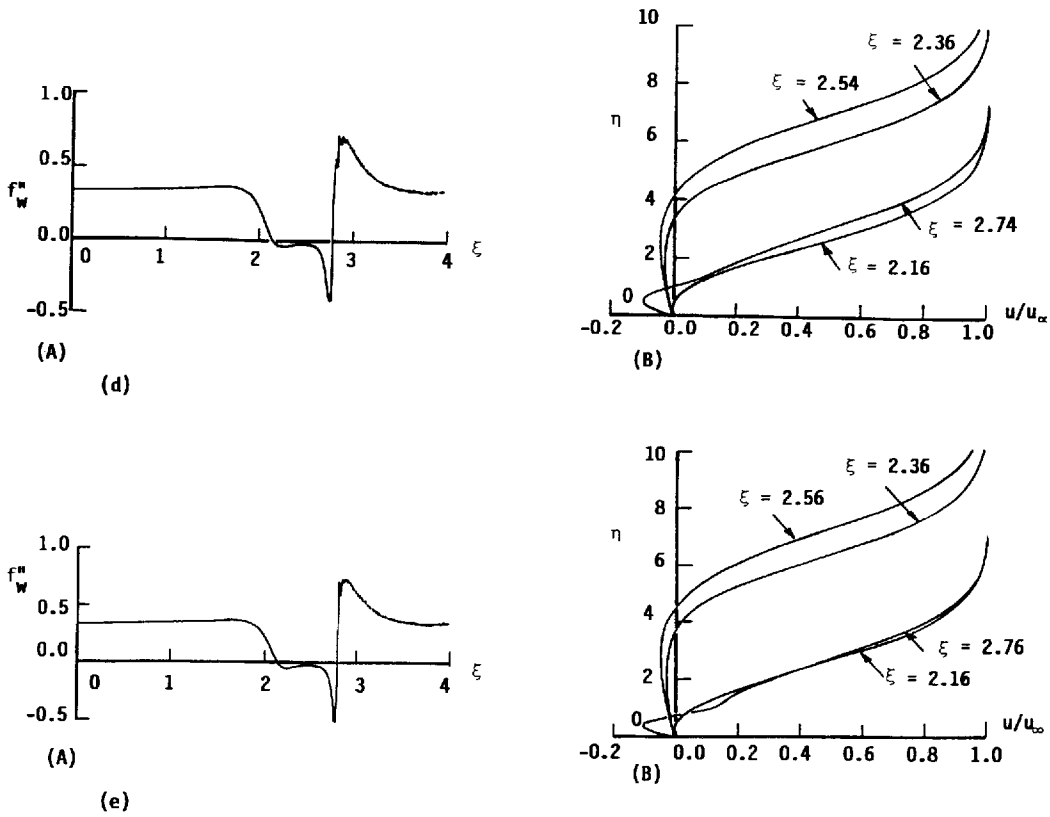

Figure 5. (Continued)

Table II. Separation, reattachment, and transition location for transitional and turbulent flow over an indented plate

R	Separation location	Reattachment location	Transition location
2×10^5	2·20	2·64	2·50
$3{\cdot}6 \times 10^5$	2·18	2·54	2·38
5×10^5	2·20	2·48	2·36
6×10^5	2·22	2·44	2·30

2.3. Turbulent flow calculations

The conjecture of the previous section was tested by performing calculations which involved the transitional and turbulence model and sweeps were necessary to ensure that upstream effects of the transitional and turbulent flows were properly represented.

Calculations of this type were performed and a sample of the results is shown in Figure 6. The resulting transition locations are shown in Table II and it is clear that they deviate increasingly from those of Table I as the Reynolds number was increased by comparatively small amounts.

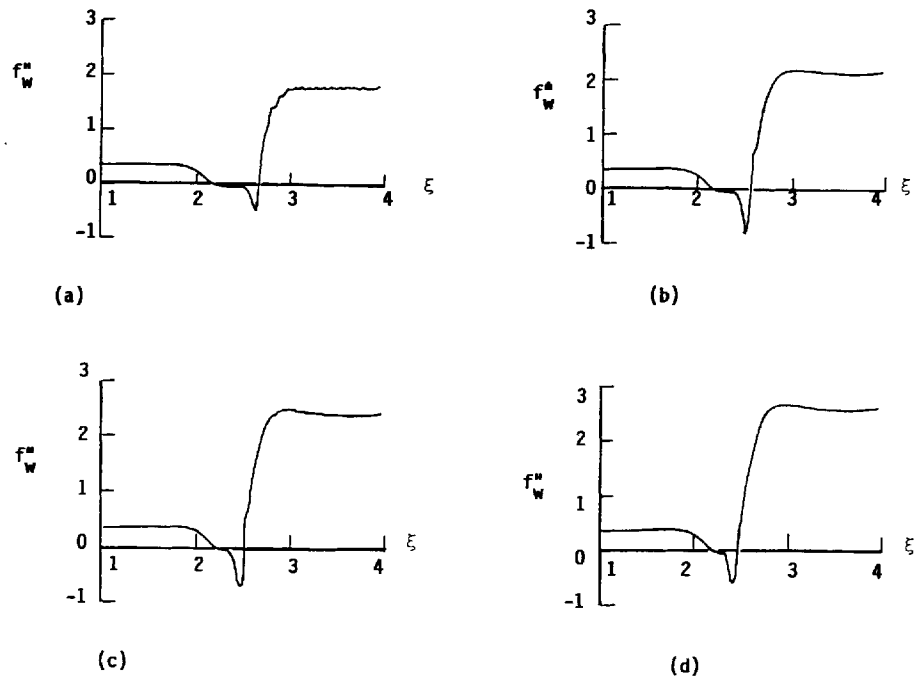

Figure 6. Variation of the dimensionless wall shear parameter for transitional–turbulent flow: (a) $R_0 = 2 \times 10^5$; (b) $R_0 = 3{\cdot}6 \times 10^5$; (c) $R_0 = 5 \times 10^5$; (d) $R_0 = 6 \times 10^5$

Figure 6 shows the variations of the wall shear and that the length of the separation bubble becomes much shorter than those shown in Figure 5 corresponding to the laminar flows at the same Reynolds number. Further comparison of the two sets of figures confirms the conjecture that the differences between laminar and transitional–turbulent flows increase with Reynolds number.

The calculations which led to Figure 6(a)–6(d) were performed without numerical problems and we can reasonably expect that calculations of this type can be performed at much higher Reynolds numbers.

3. CONCLUDING REMARKS

It is evident that two aspects of the calculations discussed in the previous three subsections may each contribute to numerical difficulties such as those experienced by Henkes and Veldman.[12] As the Reynolds numbers are increased, the recovery of the wall shear parameter becomes more rapid and achieves gradients which present problems particularly around the location of laminar reattachment. Here we have investigated the effect of step length and have shown that, consistent with the study of Rubin and his co-workers,[16,20,21] very fine grids would be required to resolve the gradients at higher Reynolds numbers. Thus, numerical accuracy does contribute to the breakdown of the solutions. At the same time, again consistent with the study of Rubin and Himansu,[16] it is clear that these breakdowns occur for laminar flows which may never exist. Our calculations have shown that the onset of transition occurs within the recirculation region for the four Reynolds numbers considered. As a consequence, we should expect that the influence of turbulent fluctuations would be present after the transition location and would increase with Reynolds number so that, at higher Reynolds numbers, we might expect that the laminar flows

calculated downstream of transition would deviate considerably from those which would exist in practice. Calculations involving laminar, transitional and turbulent flows have been performed over a more extensive Reynolds number range than those for laminar flow and confirm this conjecture. The results were obtained without any sign of numerical instability and with step lengths which were modest.

ACKNOWLEDGEMENT

This research was performed under contract No. AFOSR-90-0262 for the Department of the Air Force Office of Scientific Research (AFSC).

REFERENCES

1. D. Catherall and K. W. Mangler, 'The integration of the two dimensional laminar boundary-layer equations past the point of vanishing skin friction'. *J. Fluid Mech.*, **26,** 163–182 (1966).
2. J. M. Klineberg and J. L. Steger, 'On laminar boundary-layer separation', *AIAA Paper No. 74–94*, 1974.
3. H. P. Horton, 'Separating laminar boundary layers with prescribed wall shear', *AIAA J.*, **12,** 1772–1774 (1974).
4. W. R. Briley and H. McDonald, 'Numerical predictions of incompressible separation bubbles', *J. Fluid Mech.*, **69,** 631–656 (1975).
5. P. Crimi and B. L. Reeves, 'Analysis of leading-edge separation bubbles on airfoils', *AIAA J.*, **14,** 1548–1555 (1976).
6. O. K. Kwon and R. H. Pletcher, 'Prediction of incompressible separated boundary layers including viscous–inviscid interaction', *Trans. ASME: J. Fluids Eng.*, **101,** 466–472 (1979).
7. J. E. Carter, 'Solutions of laminar boundary layers with separation and reattachment', *AIAA Paper No. 74–583*, 1974.
8. J. E. Carter, 'Inverse solutions of laminar boundary-layer flows with separation and reattachment', *NASA TR R-447*, 1975.
9. T. Cebeci, 'Separated flows and their representation by boundary-layer equations', *CSULB Mechanical Engineering Report, ONR-CR215-234-2*, 1976.
10. J. E. Carter and S. F. Wornom, 'Solutions for incompressible separated boundary layers including viscous–inviscid interaction', *NASA SP347*, 1975, pp. 125–150.
11. A. E. P. Veldman, 'New, quasi-simultaneous method to calculate interacting boundary layers', *AIAA J.*, **154,** 79–85 (1981).
12. R. A. W. M. Henkes and A. E. P. Veldman, 'On the breakdown of the steady and unsteady interacting boundary-layer description', *J. Fluid Mech.*, **179,** 513–529 (1987).
13. A. E. P. Veldman, 'A numerical method for the calculation of laminar, incompressible boundary layers with strong viscous–inviscid interaction', *NLR TR 79023U*, 1979.
14. A. E. P. Veldman and D. Dijkstra, 'A fast method to solve incompressible boundary-layer interaction problems', *Proc. 7th Internat. Conf. on Numerical Methods of Fluid Mechanics*, Amsterdam, 1980, vol. 141, pp. 411–416.
15. D. E. Edwards and J. E. Carter, 'A quasi-simultaneous finite-difference approach for strongly interacting flow', *Proc. 3rd Symp. on Numerical and Physical Aspects of Aerodynamic Flows*, Long Beach, January 1985.
16. S. G. Rubin and A. Himansu, 'Convergence properties of high Reynolds number separated flow calculations', *Int. j. numer. methods fluids*, **9,** 1395–1411 (1989).
17. T. Cebeci, 'Numerical instabilities in the calculation of laminar separation bubbles and their implications', *AIAA J.*, **27,** 656 (1989).
18. T. Cebeci and S. M. Schimke, 'The calculation of separation bubbles in interactive turbulent boundary layers', *J. Fluid Mech.*, **131,** 305–317 (1983).
19. T. Cebeci, 'Essential ingredients of a method for low Reynolds-number airfoils', *AIAA J.*, **27,** 1680–1688 (1989).
20. S. V. Ramakrishnan and S. Rubin, 'Time consistent pressure relaxation procedure for compressible Navier–Stokes equations', *AIAA J.*, **25,** 905–913 (1987).
21. K. Srinivasan and S. Rubin, 'Adaptive multigrid domain decomposition solutions of the reduced Navier–Stokes equations', *Proc. 6th SIAM Domain Decomposition Symposium*, Norfolk, VA, May 1991.
22. T. Cebeci and A. M. O. Smith, *Analysis of Turbulent Boundary Layers*, Academic Press, New York, 1974.
23. P. Bradshaw, T. Cebeci and J. H. Whitelaw, *Engineering Calculation Methods for Turbulent Flows*, Academic Press, New York, 1981.
24. J. A. Majeski, 'Indented plate problem revisited', *M.S. Thesis*, Department of Aerospace Engineering, California State University, Long Beach, 1990.